

Self-Assembly of Multinuclear Coordination Species with Chiral Bipyridine Ligands: Silver Complexes of 5,6-CHIRAGEN(*o,m,p*-xylydene) Ligands and Equilibrium Behaviour in Solution

Olimpia Mamula,^[a] Florence J. Monlien,^[b] Alain Porquet,^[b] Gérard Hopfgartner,^[c] André E. Merbach,^[b] and Alex von Zelewsky*^[a]

Abstract: The complexation reactions between Ag⁺ and a series of enantiopure ligands belonging to the CHIRAGEN (from CHIRality GENerator) family (**L1**, **L2**, **L3**, based on (–)-5,6-pinene bipyridine) have been studied in solution. It has been shown that the length of the bridge plays a fundamental role in the self-assembly processes leading to different compounds: mononuclear complexes (with **L3**), mixtures of polynuclear complexes (with **L2**) and circular helicates (with **L1**). Although the absolute configuration of the chiral centres in all three ligands is the same, the metal-centred chirality of **L3** (*A*) is

inverted with respect to that in the other two complexes with **L1** and **L2** (*A*). The metal configuration is thus opposite in the mononuclear complex with respect to the polynuclear species. Detailed thermodynamic studies were carried out for the Ag⁺ and **L1** ligand system by ¹H and ¹⁰⁹Ag NMR spectroscopy (as a function of concentration, temperature and pressure). At low temperature and high pressure, the [Ag₆**L1**]⁶⁺ hexa-

Keywords: helical structures • N ligands • NMR spectroscopy • silver • thermodynamics

nuclear circular helicate forms a tetranuclear circular helicate [Ag₄**L1**]⁴⁺: 2[Ag₆**L1**]⁶⁺ ⇌ 3[Ag₄**L1**]⁴⁺. The thermodynamics parameters, obtained by temperature and pressure variation, have the following values: $K^{298} = (8.7 \pm 0.7) \times 10^{-5} \text{ mol kg}^{-1}$, $\Delta H^\circ = -15.65 \pm 0.8 \text{ kJ mol}^{-1}$, $\Delta S^\circ = -130.2 \pm 3 \text{ J mol}^{-1} \text{ K}^{-1}$ and $\Delta V^\circ(256 \text{ K}) = -160 \pm 12 \text{ cm}^3 \text{ mol}^{-1}$. The reaction volume calculated according to Connolly's method indicates that the calculated structure of [Ag₄**L1**]⁴⁺ is plausible. Both the signs and large magnitudes of ΔS° and ΔV° are counterintuitive, yet can be understood by modelling methods.

Introduction

Self-assembly of coordination species has recently attracted much attention.^[1] Ag⁺ represents a labile coordination centre that often yields well-defined species in such reactions. Helicates^[2–5] have been preferred target objects in these reactions, because of their interesting properties^[6–8] or for the further construction of special architectures, for example, molecular knots.^[9, 10] Both prevalent coordination geometries of metal centres, tetrahedral (T-4) and octahedral (OC-6), can

give rise to helical structures. Since helicates are intrinsically chiral objects, it is an especially interesting challenge to select self-assembling systems that yield helicates in a predetermined configuration. We have recently shown that the family of CHIRAGEN (from CHIRality GENerator) ligands 4,5-CHIRAGEN(*m*-xylydene), based on (–)-4,5-pinene bipyridine, yields configurationally predetermined triple-stranded helicates with octahedral coordination centres.^[11] From reaction with tetrahedral metal centres (Ag⁺), the sterically more demanding 5,6-CHIRAGENS (Scheme 1) yield a variety of helical architectures depending on the geometry of the bridge. Three of these helical structures have been elucidated in the solid state by X-ray diffraction.^[12, 13]

Solution behaviour of enantiopure helicates^[14] has been studied in several cases. Yet thermodynamic parameters were not determined. The solid composition of [Ag₆**L1**](PF₆)₆, which can be crystallized, has been shown to contain a 6+ charged cation of a unique circular monostranded helicate with predetermined chirality (Figure 1).

Of special interest is the problem whether the self-assembly of a distinct species is already accomplished in solution, or whether it is a solid-state property of the particular composition of matter. In the present publication, we report the

[a] Prof. A. von Zelewsky, Dr. O. Mamula
Department of Chemistry, University of Fribourg
Pérolles, 1700, Fribourg (Switzerland)
Fax (+41)26-3009738
E-mail: alexander.vonzewelsky@unifr.ch

[b] F. J. Monlien, Dr. A. Porquet, Prof. A. E. Merbach
Institut de Chimie Minérale et Analytique
Université de Lausanne BCH, 1015 Lausanne (Switzerland)

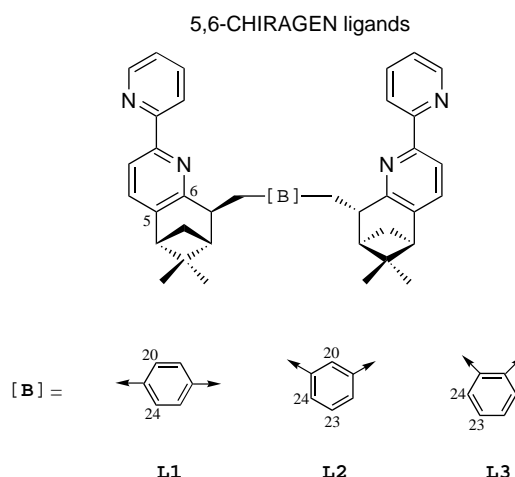
[c] Dr. G. Hopfgartner
F. Hoffmann-La Roche, Pharmaceuticals Division
Department of Drug Metabolism and Kinetics
4070 Basel (Switzerland)

Supporting information for this article is available on the WWW under <http://www.wiley-vch.de/home/chemistry/> or from the author.

results of detailed investigations of the solution behaviour of the circular helicates as well as the complexation studies of newly reported ligands, the 5,6-CHIRAGEN(xyliden) series.

Abstract in French: Les réactions de complexation entre l'argent(I) et une série de ligands énantiomériquement purs (**L1**, **L2** et **L3**) appartenant à la famille des CHIRAGEN, ont été étudiées en solution. Il a été démontré que la longueur du pont joue un rôle fondamental dans les processus d'auto-assemblage en conduisant à la formation de différents composés: complexe mononucléaire (avec **L3**), mélange de complexes polynucléaires (avec **L2**) et hélicates circulaires (avec **L1**). Bien que la configuration absolue des centres chiraux des trois ligands soit la même, le centre de chiralité du complexe formé avec **L3** (Δ), situé sur le métal, est inversé par rapport à ceux des complexes formés avec **L1** et **L2** (Λ). La configuration du métal pour le complexe mononucléaire est par conséquent, opposée à celles des espèces polynucléaires. Des études thermodynamiques détaillées en RMN ^1H et ^{109}Ag (variation de concentration, de température et de pression) ont été menées sur le système impliquant Ag^+ avec le ligand **L1**. Les résultats obtenus démontrent que le complexe $[\text{Ag}_6\text{L1}_6]^{6+}$ forme à basse température et à haute pression l'hélicate tétranucléaire circulaire $[\text{Ag}_4\text{L1}_4]^{4+}$ selon l'équilibre: $2[\text{Ag}_6\text{L1}_6]^{6+} \rightleftharpoons 3[\text{Ag}_4\text{L1}_4]^{4+}$. Les paramètres thermodynamiques suivants ont été obtenus à température et pression variable: $K^{298} = (8.7 \pm 0.7) \cdot 10^{-5} \text{ mol kg}^{-1}$, $\Delta H^\circ = -15.65 \pm 0.8 \text{ kJ mol}^{-1}$, $\Delta S^\circ = -130.2 \pm 3 \text{ J mol}^{-1} \text{ K}^{-1}$ et $\Delta V^\circ(256 \text{ K}) = -160 \pm 12 \text{ cm}^3 \text{ mol}^{-1}$. Le volume de réaction calculé suivant la méthode de Connolly, montre que la structure calculée pour $[\text{Ag}_4\text{L1}_4]^{4+}$ est vraisemblable. Le signe tout comme les grandes valeurs de l'entropie et du volume de réaction sont inattendus, mais explicables par la modélisation.

Abstract in Romanian: Au fost studiate în soluție reacțiile de complexare între Ag^+ și trei liganzi enantiopuri (**L1**, **L2**, **L3**) de tip CHIRAGEN. S-a arătat că lungimea punții are un rol esențial în procesele de autoasamblare, conducând la compuși diferiți: complecși mononucleari (cu **L3**), amestecuri de complecși polinucleari (cu **L2**) și helicați circulari (cu **L1**). Deși configurația absolută a centrilor chirali din cei trei liganzi este aceeași, chiralitatea la centrul metalic în cazul compușilor lui **L3** (Δ) este inversată comparativ cu cea din complecșii cu liganzii **L2** și **L3** (Λ). Studii termodinamice detaliate au fost efectuate în cazul sistemului conținând Ag^+ și liganzul **L1**, utilizând ^1H RMN și ^{109}Ag RMN în funcție de concentrație, temperatură și presiune. S-a constatat că helicalul circular hexanuclear $[\text{Ag}_6\text{L1}_6]^{6+}$ formează la temperatură joasă și presiune ridicată helicalul circular tetranuclear $[\text{Ag}_4\text{L1}_4]^{4+}$, așa cum o arată echilibrul: $2[\text{Ag}_6\text{L1}_6]^{6+} \rightleftharpoons 3[\text{Ag}_4\text{L1}_4]^{4+}$. Parametrii termodinamici obținuți prin variația temperaturii și a presiunii au valorile: $K^{298} = (8.7 \pm 0.7) \cdot 10^{-5} \text{ mol g}^{-1}$, $\Delta H^\circ = -15.65 \pm 0.8 \text{ J mol}^{-1}$, $\Delta S^\circ = -130.2 \pm 3 \text{ J mol}^{-1} \text{ K}^{-1}$ și $\Delta V^\circ(256 \text{ K}) = -160 \pm 12 \text{ cm}^3 \text{ mol}^{-1}$. Volumul de reacție obținut prin metoda Connolly arată că structura calculată pentru $[\text{Ag}_4\text{L1}_4]^{4+}$ este plauzibilă. Semnul, ca și valorile mari ale entropiei și ale volumului de reacție sunt neașteptate dar pot fi explicate prin modelizare.



Scheme 1.

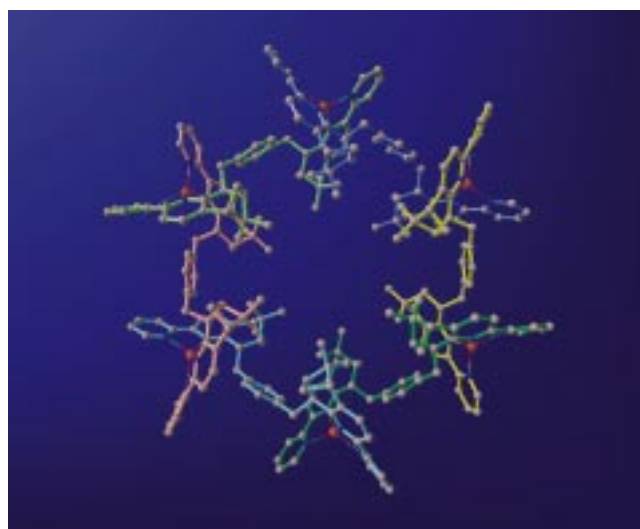


Figure 1. X-ray structure of the cation $[\text{Ag}_6\text{L1}_6]^{6+}$.^[12]

Results and Discussion

The synthesis of the various ligands that are representatives of the 5,6-CHIRAGEN family, based on (–)-5,6-pinene bipyridine, is straightforward.^[15, 16] The silver complexes of **L1**, **L2** and **L3** are obtained quantitatively by the reaction of a 1:1 mixture of AgPF_6 in CH_3CN and the ligand dissolved in CHCl_3 .

Influence of the bridge: One of the interesting aspects of the CHIRAGEN ligand family is its variability in terms of geometry of the bridging unit. In the present case this means that all three isomers *para*, *meta* and *ortho*-xylidene can be used. The main emphasis was given to the investigations on the self-assembly of the *para*-xylidene-bridged ligand (**L1**), the only one for which a crystal structure analysis could be carried out showing the presence of a circular monostranded helicate.

The ES-MS spectrum indicates formation of polynuclear species with **L2**. The most abundant species corresponds to the dinuclear complex $[\text{Ag}_2\text{L2}_2]^{2+}$, but signals of lower

intensity corresponding to $[\text{Ag}_3\text{L}_2]^{3+}$ and $[\text{Ag}_5\text{L}_2]^{5+}$ were detected (see Experimental Section). At room temperature broad signals are observed in the ^1H NMR spectrum. At lower temperatures (below 253 K) a large number of narrow signals are observed, an indication of a distribution of several complex species. Ligand **L3** shows a completely different behaviour to that of **L1** and **L2**. The ES-MS spectrum reveals mainly the presence of the mononuclear complex $[\text{AgL}_3]^+$. Its ^1H NMR spectrum is well resolved at all temperatures (see Supporting Information). The C_2 symmetry of the ligand is preserved upon complexation (the number of signals is half the number of proton in the ^1H NMR spectrum). Molecular models (Figure 2) show that **L3** can easily occupy all four ligand sites of a tetrahedrally coordinated Ag^+ centre, thus yielding a complex $[\text{AgL}_3]^+$ that is related to the mononuclear complex obtained with the 5,6-CHIRAGEN[0] (ligand without bridge).^[17]

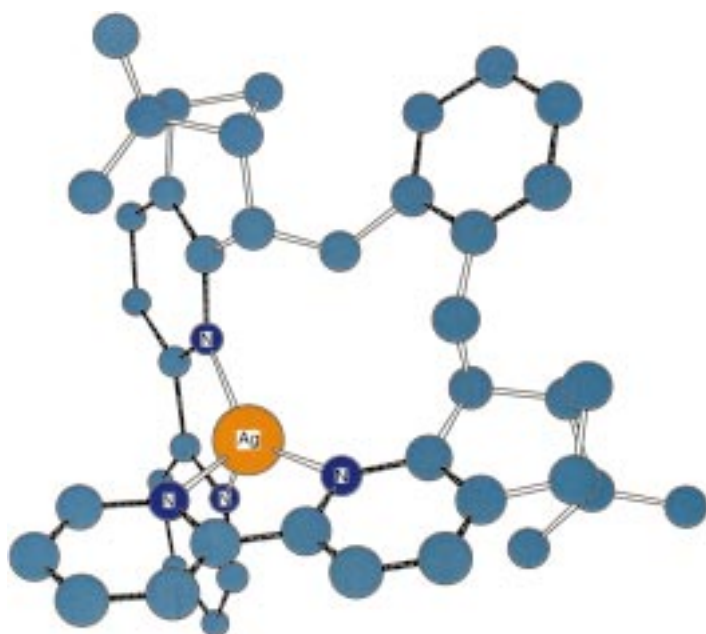


Figure 2. Chem 3D model of the mononuclear complex $[\text{AgL}_3]^+$.

The CD spectra of the three complexes (Figure 3) have opposite signs ($\Delta\epsilon > 0$ for **L1** and **L2**, while $\Delta\epsilon < 0$ for **L3** at ca. 315 nm) of the two exciton coupled $\pi-\pi^*$ transitions in the bpy moieties. Considering that the chirality of the metal centres determined by X-ray in the complex with **L1** was Δ , we assume that the same Δ chirality of the metal centres is present also in the complexes with **L2**, and that it is Δ in the mononuclear species with **L3**. The chirality of the metal centre in complexes with **L3** is in accordance with that determined for the sterically related ligand, 5,6-CHIRAGEN[0], and measured by X-ray diffraction.^[17]

Equilibrium behaviour: It has already been reported that for the circular helicate $[\text{Ag}_6(\text{L1})_6](\text{PF}_6)_6$, all signals of the aromatic protons are shifted with respect to the free ligand and some of them are also broadened significantly at room temperature.^[12] Lowering the temperature (down to 233 K in CD_3CN) shows further broadening of the NMR signals

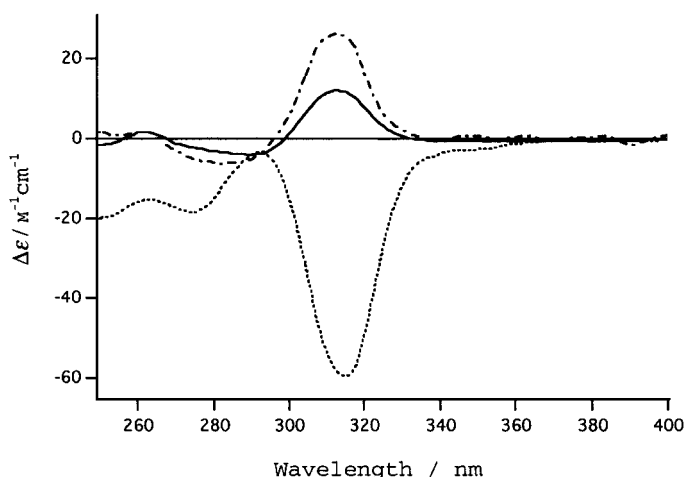


Figure 3. CD spectra of the complexes of Ag^+ with **L1** (—), **L2** (---) and **L3** (····) at 298.1 K.

leading eventually to a splitting into two sets of signals of unequal intensity. This behaviour was attributed to the existence of two rapidly exchanging species in solution.

To clarify this observation we have investigated silver helicate solutions by ^1H NMR spectroscopy as a function of concentration of Ag^+ and $[\text{Ag}_6\text{L1}_6]^{6+}$, of temperature and pressure, as well as by ^{109}Ag NMR spectroscopy.

Addition of Ag^+ to the solution of $[\text{Ag}_6\text{L1}_6]^{6+}$ (up to ca. ten equivalents) was performed at room temperature, and after five minutes at 298 K, spectra were recorded at 223 K. This treatment did not lead to any observable change in the relative proportions and chemical shifts of both species in the ^1H NMR spectrum. After addition of ca. ten equivalents of Ag^+ , solubility problems occurred and no experiment could be performed. This is a strong indication that the ratio between Ag^+ and **L1** is the same in both species in equilibrium.

To elucidate the nature of this equilibrium, we measured ^1H NMR spectra as a function of total concentration of $[\text{Ag}_6\text{L1}_6]^{6+}$ at 243 K. At this temperature the two singlets (Figure 4, zoom $\delta = 5-6$) due to the H20, H24 protons in the

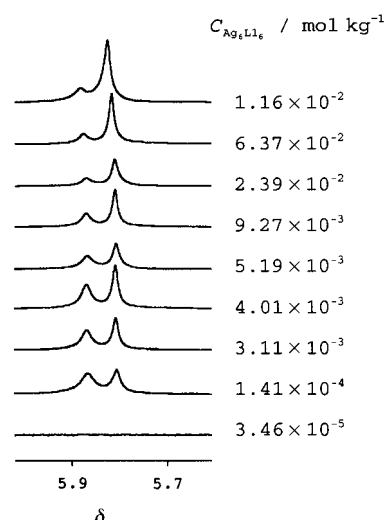


Figure 4. 400 MHz ^1H NMR spectra of a $[\text{Ag}_6\text{L1}_6](\text{PF}_6)_6$ in CD_3CN at 253 K from a concentration $C_{\text{Ag}_6\text{L1}_6}$ of 1.16×10^{-2} to 3.46×10^{-5} mol kg^{-1} .

para-xylylene bridge, are conveniently separated and were used to obtain the best model for the equilibrium. The shifts, line-widths and relative intensities were obtained from two Lorentzian fitting procedures by using NMRICMA program.^[18]

A systematic search for equilibria of the type $n[\text{Ag}_m\text{L}_1\text{L}_m]^{m+} \rightleftharpoons m[\text{Ag}_n\text{L}_1\text{L}_n]^{n+}$, by using the relative concentration values from the NMR spectra obtained at different total concentrations yielded $n = 4$, $m = 6$ as the only numbers for which Q is a constant, $Q = \frac{[[\text{Ag}_n\text{L}_1\text{L}_n]^{n+}]^m}{[[\text{Ag}_m\text{L}_1\text{L}_m]^{m+}]^n}$

Therefore the model for which the equilibrium value was constant (Table 1) for all concentration dependence experiments is given by Equation (1) and the equilibrium constant by Equation (2).



$$K = \frac{[[\text{Ag}_4\text{L}_1\text{L}_4]^{4+}]^3}{[[\text{Ag}_6\text{L}_1\text{L}_6]^{6+}]^2} \quad (2)$$

Table 1. Proton mole fractions X and equilibrium constant K as a function of dilution^[a] in CD_3CN at 243 K.

Dilution	$C_{\text{Ag}_6\text{L}_1\text{L}_6}$ [mol kg ⁻¹]	$X_{\text{Ag}_6\text{L}_1\text{L}_6}$ [±0.03]	$X_{\text{Ag}_4\text{L}_1\text{L}_4}$ [±0.03]	log K ^[b]
1.0	1.16×10^{-2}	0.80	0.20	-3.31 ± 0.18
1.8	6.37×10^{-3}	0.76	0.24	-3.29 ± 0.14
4.9	2.39×10^{-3}	0.68	0.32	-3.24 ± 0.09
12.6	9.27×10^{-4}	0.61	0.39	-3.30 ± 0.06
22.4	5.19×10^{-4}	0.53	0.47	-3.19 ± 0.04
29.0	4.01×10^{-4}	0.47	0.53	-3.04 ± 0.02
37.4	3.11×10^{-4}	0.45	0.55	-3.06 ± 0.01
82.6	1.41×10^{-4}	0.37	0.63	-3.06 ± 0.01

[a] $m_{\text{Ag}_6\text{L}_1\text{L}_6} = 27.4$ mg in 0.459 g CD_3CN . [b] $K = \frac{[[\text{Ag}_4\text{L}_1\text{L}_4]^{4+}]^3}{[[\text{Ag}_6\text{L}_1\text{L}_6]^{6+}]^2}$.

In Equation (2) $[[\text{Ag}_6\text{L}_1\text{L}_6]^{6+}] = X_{\text{Ag}_6\text{L}_1\text{L}_6} C_{\text{Ag}_6\text{L}_1\text{L}_6}$ and $[[\text{Ag}_4\text{L}_1\text{L}_4]^{4+}] = (6/4)X_{\text{Ag}_4\text{L}_1\text{L}_4} C_{\text{Ag}_6\text{L}_1\text{L}_6}$ ($X_{\text{Ag}_6\text{L}_1\text{L}_6}$: mole fraction of the H20, H24 protons signal of the $[\text{Ag}_6\text{L}_1\text{L}_6]^{6+}$ species; $X_{\text{Ag}_4\text{L}_1\text{L}_4}$: mole fraction of the H20, H24 protons signal of the $[\text{Ag}_4\text{L}_1\text{L}_4]^{4+}$ species; $C_{\text{Ag}_6\text{L}_1\text{L}_6}$: total concentration of dissolved $[\text{Ag}_6\text{L}_1\text{L}_6](\text{PF}_6)_6$).

Log Q is constant within experimental error (within a range of ±5%). Log Q values below a total concentration of about 4×10^{-4} mol kg⁻¹ show a systematic deviation and some very broad signals of the free ligand are observed in solution. At high dilution the values tend to become significantly lower, indicating a further dissociation of the polynuclear complexes. ES-MS spectra show beside the hexanuclear and tetranuclear species also fragments formed through successive loss of $[\text{AgL}_1]^+$ as well as PF_6^- groups.

At low temperature (221 K in CD_3CN , 51 mg complex in 1.34 g CD_3CN), the ¹⁰⁹Ag NMR spectrum (Figure 5) shows two singlets at $\delta = 224$ ($[\text{Ag}_6\text{L}_1\text{L}_6]^{6+}$) and $\delta = 249$ ($[\text{Ag}_4\text{L}_1\text{L}_4]^{4+}$) relative to a AgNO_3 solution (2 M, external reference). The relative proportions of these peaks are (77 ± 3)% and (23 ± 3)% for the $\delta = 224$ and 249 signals, respectively. In the ¹⁰⁹Ag NMR spectra there is a very small shift difference, which reflects similar structural features. Even solutions of different concentrations of the same species, for example, AgNO_3 , give similar shift differences as reported by Popov et al.^[19] The corresponding log K value (-3.28 ± 0.22 mol kg⁻¹) is in

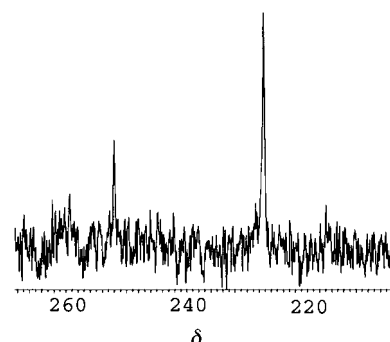


Figure 5. 27.94 MHz ¹⁰⁹Ag NMR spectrum of a $[\text{Ag}_6\text{L}_1\text{L}_6](\text{PF}_6)_6$ at 221 K ($C_{\text{Ag}_6\text{L}_1\text{L}_6} = 4.45 \times 10^{-2}$ mol kg⁻¹, 51 mg in 1.34 g CD_3CN), repetition delay: 50 s, number of scans: 1024, sweep width: 125 KHz, line broadening: 3 Hz.

a good agreement with data obtained from the temperature variation.

If we increase the temperature by 7 K, the number of scans must be doubled to obtain a spectrum owing to unfavourable longitudinal relaxation rate at higher temperature. At room temperature, no signal is observed except for the reference. The addition of free Ag^+ does not affect the relative concentration of the two species in equilibrium. This result is in good agreement with the proposed equilibrium model.

The temperature dependence of the ¹H NMR spectra was measured from 218 K up to 298 K in CD_3CN in order to obtain the thermodynamic parameters ΔH° and ΔS° of the equilibrium in Equation (1). The intensity of the signal assigned to the minor species $[\text{Ag}_4\text{L}_1\text{L}_4]^{4+}$ decreases reversibly with increasing temperature. Both signals show an expected viscosity-related decrease in line-width up to 240 K. Above this temperature, both of the signals start to broaden; this could be due to an intermolecular exchange of the metal helicates with, for example, traces of free ligand, but no kinetic data could be extracted. However, the shape of the signals of both helicates can easily be fitted, up to 270 K leading to the temperature dependence of K (Table 2).

In addition to the proton signals of the aromatic bridge, all other helicate signals show a similar reversible variable temperature dependence. The equilibrium constants were least squares fitted to Equation (3) leading to the following values: $K^{298} = (8.7 \pm 0.7) \times 10^{-5}$ mol kg⁻¹, $\Delta H^\circ = -15.65 \pm 0.8$ kJ mol⁻¹ and $\Delta S^\circ = -130.2 \pm 3$ J mol⁻¹ K⁻¹.

$$\ln K = +\Delta S^\circ/R - \Delta H^\circ/(RT) \quad (3)$$

Table 2. Proton mole fractions X and equilibrium constant K as a function of temperature in CD_3CN ($C_{\text{Ag}_6\text{L}_1\text{L}_6} = 5.57 \times 10^{-3}$ mol kg⁻¹).^[a]

T [K]	$1/T$ [10 ⁻³ K ⁻¹]	$1/T_2$ ($\text{Ag}_6\text{L}_1\text{L}_6$) [s ⁻¹]	$1/T_2$ ($\text{Ag}_4\text{L}_1\text{L}_4$) [s ⁻¹]	$X_{\text{Ag}_6\text{L}_1\text{L}_6}$ [±0.03]	$X_{\text{Ag}_4\text{L}_1\text{L}_4}$ [±0.03]	log K ^[b]
270.1	3.70	24.0	79.3	0.82	0.18	-3.78 ± 0.20
258.2	3.87	13.7	41.1	0.80	0.20	-3.61 ± 0.17
250.9	3.98	11.9	22.4	0.80	0.20	-3.60 ± 0.17
236.6	4.22	10.8	15.2	0.76	0.24	-3.32 ± 0.14
233.0	4.29	11.7	14.8	0.75	0.25	-3.30 ± 0.13
228.4	4.38	12.1	14.4	0.74	0.26	-3.23 ± 0.12
218.0	4.58	16.8	20.6	0.71	0.29	-3.06 ± 0.11

[a] $m_{\text{Ag}_6\text{L}_1\text{L}_6} = 13.9$ mg in 0.4857 g CD_3CN . [b] $K = \frac{[[\text{Ag}_4\text{L}_1\text{L}_4]^{4+}]^3}{[[\text{Ag}_6\text{L}_1\text{L}_6]^{6+}]^2}$.

^1H NMR pressure-dependence experiments were performed at 256.4 K in order to determine the reaction volume ΔV° . Figure 6 shows the pressure effect on the equilibrium in Equation (1). Because this effect is remarkably large, a small

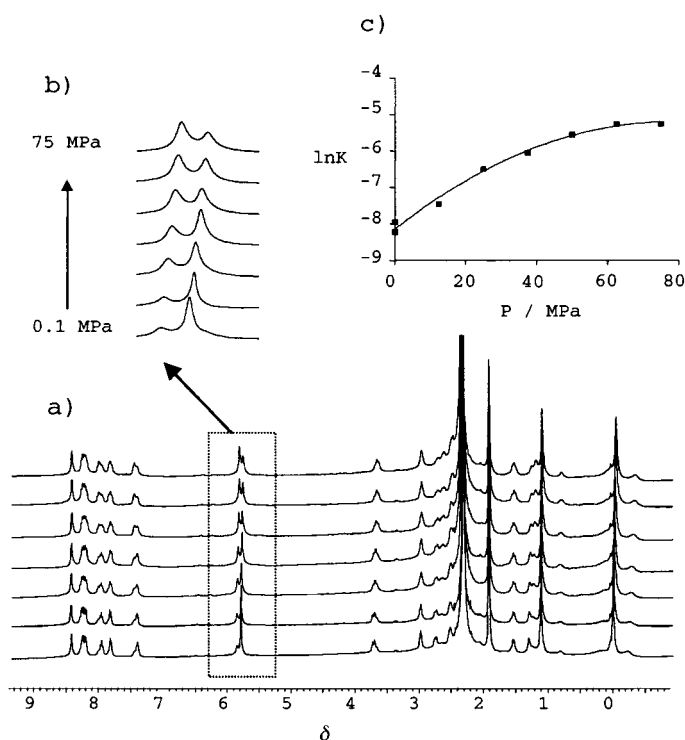


Figure 6. a) Variable pressure 400 MHz NMR spectra of a $[\text{Ag}_6\text{L16}](\text{PF}_6)_6$ at 256.4 K (13.4 mg in 1.40 g CD_3CN). b) Representation of partial NMR spectra in the δ range 5.2 to 6.3. c) The $\ln K$ pressure dependence at 256.4 K. The data points represent experimental values, while the calculated function is given as a solid line.

pressure range (75 MPa) was sufficient to obtain the reaction volume ΔV° with good accuracy. The pressure-dependence data were least-squares fitted (Figure 6c) by using Equation (4), in which K_0 is the equilibrium constant at zero pressure, ΔV° the reaction volume and $\Delta\beta^\circ$ the compressibility coefficient.

$$\ln K_p = \ln K_0 - (\Delta V^\circ P/RT) + (\Delta\beta^\circ P^2/RT) \quad (4)$$

The obtained molar reaction volume ΔV° is $-160 \pm 12 \text{ cm}^3 \text{ mol}^{-1}$ with $K_0^{256} = (2.8 \pm 0.2) \times 10^{-3} \text{ mol kg}^{-1}$ and $\Delta\beta^\circ = -(4.0 \pm 0.6)10^{-3} \text{ cm}^3 \text{ mol}^{-1} \text{ MPa}^{-1}$. This surprising result shows that the entropy decreases for a reaction in which the numbers of molecules increases and the volume decreases when going from two hexamers to three tetramers. In order to understand this unexpected result and to better visualize this phenomenon, we carried out model calculations. If we consider the chemical reaction in solution [Eq. (1)], we can define the reaction volume ΔV° by Equation (5).

$$\Delta V^\circ = -RT(\partial \ln K/\partial P)_T = \Sigma V_{\text{products}}^\circ - \Sigma V_{\text{reactants}}^\circ \quad (5)$$

With our system Equation (5) becomes Equation (6).

$$\Delta V^\circ = 3V_{\text{Ag}_4\text{L14}}^\circ - 2V_{\text{Ag}_6\text{L16}}^\circ \quad (6)$$

The X-ray structure for $[\text{Ag}_6\text{L16}]^{6+}$ is well known and its volume can be estimated in order to deduce the $[\text{Ag}_4\text{L14}]^{4+}$ volume from the reaction volume. The structure of $[\text{Ag}_4\text{L14}]^{4+}$ was minimised by using X-ray the bond lengths and constraints of $[\text{Ag}_6\text{L16}]^{6+}$.

A series of Connolly's volumes for each structure was calculated by varying the probe radius in the range of 0 to 3.0 Å. Values of 1.4–1.6 Å are usually used to mimic water solvent.^[20] Water can be considered as a spherical molecule, but this is not the case for CH_3CN . We have no accurate information of the acetonitrile solvation pattern of these complexes. Acetonitrile can interact with its N- or alkyl-tail and can stack by dipole–dipole interaction. It is difficult to define a unique value of r_{probe} for CH_3CN , so we calculated volumes with r_{probe} varying from 0.0 to 3.0 Å. The lower (≈ 1.0 Å), middle (≈ 2.0 Å) and higher (≈ 2.5 Å) values of the r_{probe} correspond to N-tail, alkyl-tail and stacking interactions, respectively. When r_{probe} is zero, the volume is defined inside the van der Waals surface.

Connolly's molecular volumes of tetramer and hexamer complexes are shown in Figure 7 (top left and top right, respectively). These calculations give the same order of magnitude for reaction volume as the experimentally observed ones, an indication that the calculated structure of $[\text{Ag}_4\text{L14}]^{4+}$ is plausible. The macroscopic molar volume increases from 1417 to 1990 $\text{cm}^3 \text{ mol}^{-1}$ for the tetramer and from 2117 to 3173 $\text{cm}^3 \text{ mol}^{-1}$ for the hexamer when r_{probe} is varied in the range from 0–3.0 Å. The reaction volume, equal to $3V_{\text{Ag}_4\text{L14}}^\circ - 2V_{\text{Ag}_6\text{L16}}^\circ$, was determined with the volume series of r_{probe} values and with the van der Waals volumes. The reaction volume calculated with Connolly's method varies non-monotonically with a maximum value of +117 and a minimum of $-375 \text{ cm}^3 \text{ mol}^{-1}$. When we calculate the ratio $3V_{\text{Ag}_4\text{L14}}^\circ/2V_{\text{Ag}_6\text{L16}}^\circ$, we observe that this variation corresponds to a variation between 1.02 and 0.94 of the volume ratio. The observed reaction volume ($-160 \pm 12 \text{ cm}^3 \text{ mol}^{-1}$) is the sum of the two contributions: the difference in the intrinsic molar volume of three tetramers and two hexamers and the difference in the solvation contribution of these species. Our modelling results show that the solvation contribution can have either sign, and it is therefore not possible to decide at this point conclusively which of the two contributions is the value of the observed reaction volume. The latter is large when compared with known reaction volumes in coordination chemistry,^[21] but is closer to the values found for systems including proteins.^[21, 22]

Conclusion

We have shown that related ligands could be tuned by using small variations in the structure of the subunits (the bridge) in order to vary their behaviour in self-assembly processes. We have also combined experimental data with theoretical calculations in order to describe an equilibrium system of enantiomerically pure circular helicates. The tetrameric species is entropically disfavoured, but is enthalpically favoured at low temperature. The ΔS° value is counter-

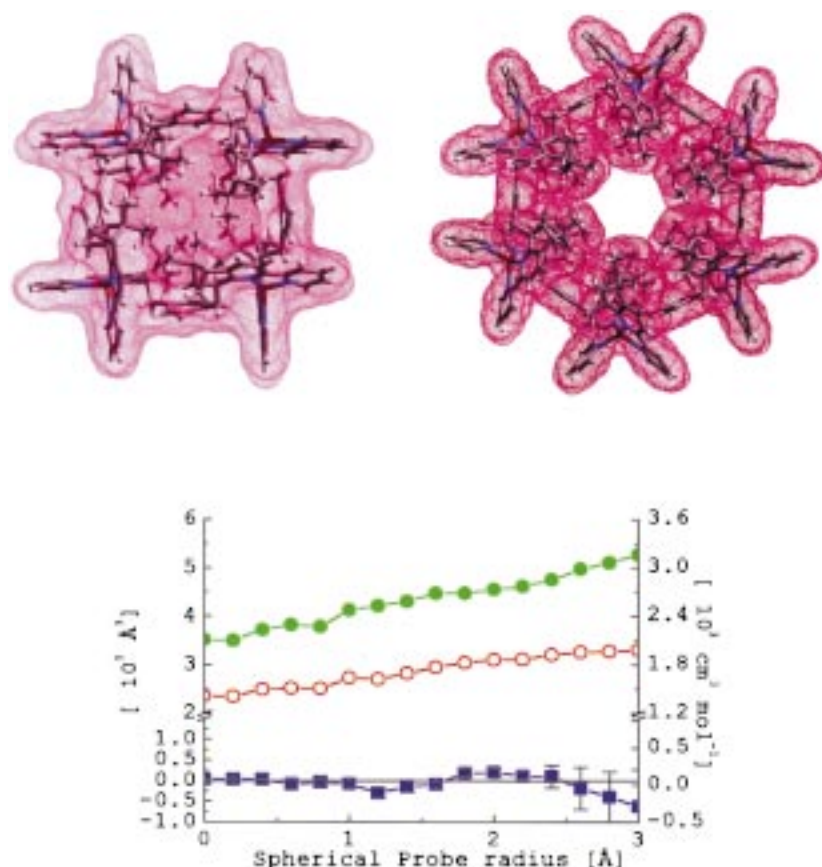
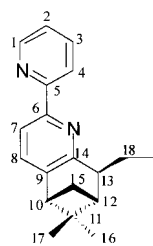


Figure 7. Top: View of the Connolly's molecular surface (in dots; left: [Ag₄L₁L₁]⁴⁺; right: [Ag₆L₁L₁]⁶⁺) for r_{probe} value equal to 1.4 Å. Bottom: Calculated molecular volume of the tetramer (open circle), of the hexamer (solid circle) and the reaction volume (solid square) as a function of the spherical probe radius (r_{probe}) over the range 0 to 3.0 Å.

intuitive, but the pressure-dependence measurement was very useful in confirming the entropy sign from isobaric investigations.

Experimental Section

Computational methods: All volume calculations were run with MSI-Cerius2 Version 3.8 package on an SGI indigo2 workstation by using the Connolly method.^[23] Details are available in the Supporting Information. All commercial chemicals were of best available grade and used without further purification. The ligand (–)-5,6-pinene bipyridine was prepared according to published procedures.^[15] All NMR spectra were recorded on DPX 600, 500 or 400 Bruker spectrometers at 27.94 MHz (¹⁰⁹Ag), 500.0 MHz (¹H) and 400.13 MHz (¹H) respectively. The ¹H chemical shift was referred to TMS and measured with respect to CH₃CN ($\delta = 1.9$) as an internal reference. CH₃CN was used as homogeneity reference. AgNO₃ was also employed as a shift and homogeneity reference for ¹⁰⁹Ag NMR experiments. The numbering scheme is given below. ¹H NMR study was performed with the following parameters: over a frequency range of



5.5 KHz, 16 K data points were acquired at a pulse length of 4.2 μ s. A larger frequency range of 27.2 KHz was used for ¹⁰⁹Ag NMR to collect 240 K data points with a pulse length of 20 μ s and an exponential line broadening of 3 Hz was subtracted in the data analysis. Bruker B-VT1000 temperature control units were used to stabilise the temperature, which was

measured (± 0.5 K) by a technical substitution.^[24] The high-pressure liquid NMR spectra were recorded with a home-built, narrow-bore, high-resolution probehead.^[25, 26] The probehead was thermostated with a fluid circulated in a double helix outside of the vessel. ES-MS measurements: the complexes were analysed in positive mode on an API III triple quadrupole mass spectrometer (PE Sciex, Concord, Toronto, Canada) equipped with an ion spray (pneumatically-assisted electrospray) source (IS-MS). The complexes were dissolved in acetonitrile at a concentration of 5 mg mL⁻¹ and infused into the MS at a flow rate between 5 and 10 μ L min⁻¹. The spectra were recorded under low up-front declustering or collision induced dissociation conditions, typically $\Delta V = 10$ V between the orifice and the first quadrupole of the mass spectrometer. Electronic spectra were measured using a Perkin-Elmer Lambda 40. CD spectra were recorded in a Jasco J-715 spectropolarimeter and the results are given in $\Delta\epsilon$ [M⁻¹ cm⁻¹].

Ligand syntheses: In a typical procedure, a Schlenk flask was charged under inert atmosphere (argon) with freshly distilled THF (15 mL) and cooled down to -20 °C (isopropyl alcohol bath). Diisopropylamine (0.34 mL, 2.4 mmol) followed by *n*-butyllithium (1.6 M in hexane, 1.35 mL, 2.2 mmol) were added by syringe. The temperature was increased to 0 °C and the solution was stirred for ten minutes at this temperature. After cooling

to -40 °C, (–)-5,6-pinene bipyridine (0.5 g, 2 mmol) dissolved in dried THF (7 mL) was added dropwise (30 minutes). The dark blue solution was stirred at -40 °C for 2 hours. Then, a solution of the corresponding α, α' -dibromoxyl compound (264 mg, 1 mmol) in THF was added slowly (30 minutes). The decolorized solution was stirred at room temperature for one hour. Then, the reaction was quenched with water (1 mL). The THF was removed, more water was added and the mixture was extracted with CH₂Cl₂. The organic phase was dried (MgSO₄) and filtered. The brown-yellow residue was purified by column chromatography using as eluant Hexane/EtOAc/TEA = 3:1:0.1, $R_f = 0.38$, yield: 84 % for **L2** and Hexane/EtAc/TEA = 2:1:0.1, $R_f = 0.4$, yield: 75 % for **L3**.

Ligand L2: ¹H-NMR (CDCl₃, 300 MHz): $\delta = 8.64$ (ddd, ³ $J_{1,2} = 4.8$ Hz, ⁴ $J_{1,3} = 1.8$ Hz, ⁵ $J_{1,4} = 0.8$ Hz, 2H; H1), 8.46 (d, ³ $J_{4,3} = 8.0$ Hz, 2H; H4), 8.12 (d, ³ $J_{7,8} = 7.7$ Hz, 2H; H7), 7.79 (ddd, ³ $J_{3,4} = 8$ Hz, ³ $J_{3,2} = 7.4$ Hz, 2H; H3), 7.35 (d, ³ $J_{8,7} = 7.7$ Hz, 2H; H8), 7.26 (s, 1H; H20), 7.23 (m, 3H; H2, H23), 7.17 (d, ³ $J_{24, 23} = 8.2$ Hz, 2H; H24), 3.85 (dd, ² $J_{18b, 18a} = 13.6$ Hz, ³ $J_{18b, 13} = 3.7$ Hz, 2H; H18b), 3.40 (ddd, ³ $J_{13, 18b} = 3.7$ Hz, ³ $J_{13, 18a} = 11.0$ Hz, ³ $J_{13, 12} = 3$ Hz, 2H; H13), 2.80 (dd, ³ $J_{10, 15b} = 5.5$ Hz, ⁴ $J_{10, 12} = 5.5$ Hz, 2H; H10), 2.72 (dd, ² $J_{18a, 18b} = 13.6$ Hz, ³ $J_{18a, 13} = 11$ Hz, 2H; H18a), 2.56 (ddd, ³ $J_{15b, 10} = 5.5$ Hz, ³ $J_{15b, 12} = 5.5$ Hz, ² $J_{15b, 15a} = 9.6$ Hz, 2H; H15b), 2.16 (ddd, ³ $J_{12, 15b} = 5.5$ Hz, ⁴ $J_{12, 10} = 5.5$ Hz, ³ $J_{12, 13} = 3$ Hz, 2H; H12), 1.45 (d, ² $J_{15a, 15b} = 9.6$ Hz, 2H; H15a), 1.34 (s, 6H; H17), 0.63 (s, 6H; H16); ¹³C NMR (CDCl₃, 75.44 MHz): $\delta = 158.74$ (q), 156.88 (q), 153.33 (q), 149.06 (C1), 142.30 (q), 141.16 (q), 136.79 (C3), 133.75 (C8), 130.24 (C20), 128.23 (C23), 126.97 (C24), 123.11 (C2), 120.90 (C4), 118.05 (C7), 47.00 (C10), 46.34 (C13), 42.71 (C12), 41.20 (q, C11), 38.78 (C18), 28.35 (C15), 26.40 (C17), 20.95 (C16); MS (FAB, *m*-nitrobenzyl alcohol): m/z (%): 603.3 (80) [M]⁺, 249.2 (85) [M – C₇H₁₇N₂]⁺, 207.2 (100); UV/Vis (0.378 mg in 25 mL CH₂Cl₂): λ_{max} (ϵ) = 228 (15700), 250 (19500), 256 (20000), 296 (36000), 313 nm (26300, sh); elemental analysis calcd (%) for C₄₂H₄₂N₄ · 0.75 H₂O: C 81.85, H 7.11, N 9.09; found: C 81.66, H 7.33, N 8.50.

Ligand L3: ^1H NMR (CDCl_3 , 300 MHz): $\delta = 8.55$ (d, $^3J_{1,2} = 4.8$ Hz, 2H; H1), 8.26 (d, $^3J_{4,3} = 8.0$ Hz, 2H; H4), 8.12 (d, $^3J_{7,8} = 7.7$ Hz, 2H; H7), 7.44 (ddd, $^3J_{3,4} = 8$ Hz, $^3J_{3,2} = 7.5$ Hz, $^4J_{3,1} = 1.8$ Hz, 2H; H3), 7.35 (m, 2H; H24), 7.30 (d, $^3J_{8,7} = 7.7$ Hz, 2H; H8), 7.23 (m, 2H; H23), 7.13 (dd, $^3J_{2,1} = 4.8$ Hz, $^3J_{2,3} = 7.4$ Hz, 2H; H2), 3.96 (dd, $^2J_{18b,18a} = 14.0$ Hz, $^3J_{18b,13} = 3.3$ Hz, 2H; H18b), 3.47 (d, $^3J_{13,18a} = 10.7$ Hz, 2H; H13), 2.97 (dd, $^2J_{18a,18b} = 14.0$ Hz, $^3J_{18a,13} = 10.7$ Hz, 2H; H18a), 2.76 (dd, $^3J_{10,15b} = 5.6$ Hz, $^4J_{10,12} = 5.6$ Hz, 2H; H10), 2.52 (ddd, $^3J_{15b,10} = 5.6$ Hz, $^3J_{15b,12} = 5.6$ Hz, $^2J_{15b,15a} = 9.7$ Hz, 2H; H15b), 2.16 (ddd, $^3J_{12,15b} = 5.6$ Hz, $^4J_{12,10} = 5.6$ Hz, 2H; H12), 1.50 (d, $^2J_{15a,15b} = 9.7$ Hz, 2H; H15a), 1.32 (s, 6H; H17), 0.61 (s, 6H; H16); ^{13}C NMR (CDCl_3 , 75.44 MHz): $\delta = 159.20$ (q), 156.88 (q), 149.23 (q), 149.03 (C1), 142.72 (q), 140.31 (q), 137.12 (C3), 133.97 (C8), 130.67 (C24), 126.22 (C23), 123.40 (C2), 121.27 (C4), 118.21 (C7), 47.29 (C10), 46.13 (C13), 43.26 (C12), 41.58 (q, C11), 35.77 (C18), 29.26 (C15), 26.70 (C17), 21.30 (C16); MS(EI): m/z (%): 603 (3) $[\text{M}+\text{H}]^+$, 602 (8) $[\text{M}]^+$, 353 (10) $[\text{M} - \text{C}_{17}\text{H}_{17}\text{N}_2]^+$, 249 (45) $[\text{M} - \text{C}_{25}\text{H}_{25}\text{N}_2]^+$, 233 (21) $[\text{M} - \text{C}_{26}\text{H}_{26}\text{N}_2]^+$, 221 (38) $[\text{M} - \text{C}_{27}\text{H}_{29}\text{N}_2]^+$, 207 (100) $[\text{M} - \text{C}_{28}\text{H}_{31}\text{N}_2]^+$, 104 (37) $[\text{M} - \text{C}_{34}\text{H}_{34}\text{N}_4]^+$, 78 (22) $[\text{py}]^+$; UV/Vis (25°C , 0.37 mg in 25 mL CH_2Cl_2): λ_{max} (ϵ) = 228 (15000), 250 (19500), 256 (20000), 296 (36000), 314 nm (26000, sh); elemental analysis calcd (%) for $\text{C}_{42}\text{H}_{42}\text{N}_4 \cdot 0.3\text{H}_2\text{O}$: C 82.94, H 7.06, N 9.21; found: C 82.92, H 7.37, N 8.85.

Complex syntheses: The ligand (62.1 mg, 0.1 mmol) dissolved in acetonitrile/chloroform 5:1 (10 mL) was added rapidly under inert atmosphere (Ar) to a solution containing AgPF_6 (25.3 mg, 0.1 mmol, Fluka) in CH_3CN (5 mL). The resulting colorless solution was stirred for few minutes, and after the removal of the solvents, a white powder was obtained that was dried under high vacuum and analysed. The analytical data of the silver complex with **L1** were published in ref. [12].

Silver(0)-L3 complex: ^1H NMR (CD_3CN , 300 MHz, 25°C): $\delta = 8.16$ (d, $^3J_{1,2} = 8.5$ Hz, 2H; H1), 8.10 (d, $^3J_{7,8} = 8.0$ Hz, 2H; H7), 7.86 (m, 4H; H3, H4), 7.74 (d, $^3J_{8,7} = 8.0$ Hz, 2H; H8), 7.17 (m, 4H; H2, H24), 7.04 (m, 2H; H23), 4.43 (d, $^2J_{18b,18a} = 13.5$, 2H; H18b), 3.63 (d, $^2J_{13,18b} = 13.0$ Hz, 2H; H13), 3.02 (dd, $^4J_{10,12} = 5.7$ Hz, $^3J_{10,15b} = 5.7$ Hz, 2H; H10), 2.80 (dd, $^2J_{18a,18b} = 13.5$ Hz, 2H; H18a), 2.70 (ddd, $^2J_{15b,15a} = 10.2$ Hz, $^3J_{15b,12} = 5.0$ Hz, $^3J_{15b,10} = 5.0$ Hz, 2H; H15b), 1.93 (m, 2H; H12), 1.76 (d, $^2J_{15a,15b} = 10.2$ Hz, 2H; H15a), 1.37 (s, 6H; H17), 0.67 (s, 6H; H16); ^{13}C NMR (CD_3CN , 75.44 MHz, 25°C): $\delta = 161.4$ (q), 153.6 (q), 151.7 (q), 150.1 (C2 or C24), 145.9 (q), 139.5 (C2 or C24), 137.7 (q), 137.2 (C8), 132.9 (C4), 127.5 (C3 or C23), 125.7 (C3 or C23), 123.1 (C1), 121.6 (C7), 47.2 (C10), 46.7 (C13), 43.8 (C18), 41.7 (q, C11), 36.6 (C12), 28.0 (C15), 26.2 (C17), 21.0 (C16); UV/Vis (CH_3CN , 2.9×10^{-4} M $[\text{AgL3}]^+$, 0.1 cm): λ_{max} (ϵ) = 259 (19000), 305 nm (26000); CD (CH_3CN , 2.9×10^{-4} M $[\text{AgL3}]^+$, 0.1 cm): λ ($\Delta\epsilon$) = 231 (−9), 292 (+9), 315 nm (+61); MS(ES) (5×10^{-3} M): m/z (%): 711.2 (100) $[\text{AgL3}]^+$, 1565.4 (10) $[\text{Ag}_2\text{L3}_2\text{PF}_6]^+$, 605.1 (3) $[\text{L3}]^+$; elemental analysis calcd (%) for $\text{AgC}_{42}\text{H}_{42}\text{N}_4\text{PF}_6$: C 58.96, H 4.95, N 6.55; found C 59.25, H 5.25, N 6.25.

Silver(0)-L2 complex: ^1H NMR: (CD_3CN , 300 MHz, 25°C ; large but distinguishable bands at room temperature): $\delta = 8.5$ (2H), 8.1 (2H), 7.9 (4H), 7.6 (2H), 7.45 (2H), 6.4 (1H), 6.2 (3H), 3.75 (d, 2H), 3.1 (2H), 2.9 (2H), 2.35 (4H), 1.6 (2H), 1.2 (8H), 0.45 (6H); a multitude (“forest”) of peaks are observed at -40°C ; UV/Vis (CH_3CN , 1.17×10^{-4} M $[\text{AgL2}]^+$, 0.1 cm): λ_{max} (ϵ) = 254 (22000), 299 (29000), 306 nm (27000, sh); CD (CH_3CN , 1.17×10^{-4} M $[\text{AgL2}]^+$, 0.1 cm): λ ($\Delta\epsilon$) = 227 (−13), 282 (−7), 314 nm (+26); MS(ES) (5×10^{-3} M): m/z (%): 711.2 (100) $[\text{AgL2}]^+$, 1566.5 (20) $[\text{Ag}_2\text{L2}_2\text{PF}_6]^+$; other signals of intensity lower than 5%: 924.7 $[\text{Ag}_3\text{L2}_3\text{PF}_6]^{2+}$, 1281.2 $[\text{Ag}_3\text{L2}_3(\text{PF}_6)_2]^{3+}$, 2421.7 $[\text{Ag}_3\text{L2}_3(\text{PF}_6)_2]^+$; elemental analysis calcd (%) for $\text{AgC}_{42}\text{H}_{42}\text{N}_4\text{PF}_6 \cdot 0.5\text{H}_2\text{O}$: C 58.34, H 5.01, N 6.48; found C 58.3, H 5.06, N 6.18.

Acknowledgement

The authors thank Prof. C. W. Schlapfer for helpful discussions and calculations. Financial support for this research provided by the Swiss National Science Foundation is acknowledged.

- [1] J.-M. Lehn, *Supramolecular Chemistry—Concepts and Perspectives*, VCH, Weinheim, **1995**.
- [2] C. Piguet, G. Hopfgartner, G. Bernardinelli, *Chem. Rev.* **1997**, *97*, 2005.
- [3] E. C. Constable, in *Comprehensive Supramolecular Chemistry*, Vol. 9 (Eds.: J.-P. Sauvage, W. Hosseini), Pergamon, Oxford, **1996**, Chapter 6.
- [4] A. F. Williams, *Chem. Eur. J.* **1997**, *3*, 9; B. Hasenknopf, J.-M. Lehn, N. Boumediene, A. Dupont-Gervais, A. van Dorsselaer, B. Kneisel, D. Fenske, *J. Am. Chem. Soc.* **1997**, *119*, 10956.
- [5] C. Provent, A. F. Williams, in *Transition Metals in Supramolecular Chemistry* (Ed. J.-P. Sauvage), Wiley, Chichester, **1999**, pp. 137–192.
- [6] A. El-ghayoury, L. Douce, A. Skoulios, R. Ziessel, *Angew. Chem.* **1998**, *110*, 2327; *Angew. Chem. Int. Ed.* **1998**, *37*, 2205.
- [7] L. Zelikovich, J. Libman, A. Shanzher, *Nature* **1995**, *374*, 790.
- [8] C. Piguet, J.-C. Buenzli, *Chem. Soc. Rev.* **1999**, *28*, 347.
- [9] G. Rapenne, C. O. Dietrich-Buchecker, J. P. Sauvage, *J. Am. Chem. Soc.* **1999**, *121*, 994.
- [10] C. O. Dietrich-Buchecker, J. P. Sauvage, A. DeCian, J. Fischer, *J. Chem. Soc. Chem. Commun.* **1994**, 2231.
- [11] H. Muerner, A. von Zelewsky, G. Hopfgartner, *Inorg. Chim. Acta* **1998**, *271*, 36.
- [12] O. Mamula, A. von Zelewsky, G. Bernardinelli, *Angew. Chem.* **1998**, *110*, 301; *Angew. Chem. Int. Ed.* **1998**, *37*, 289.
- [13] a) O. Mamula, A. von Zelewsky, T. Bark, G. Bernardinelli, *Angew. Chem.* **1999**, *111*, 3129; *Angew. Chem. Int. Ed.* **1999**, *38*, 2945; b) O. Mamula, A. von Zelewsky, T. Bark, H. Stoeckli-Evans, unpublished results.
- [14] C. Provent, E. Rivara-Minten, S. Hewage, G. Brunner, A. F. Williams, *Chem. Eur. J.* **1999**, *5*, 3487.
- [15] P. Hayoz, A. von Zelewsky, *Tetrahedron Lett.* **1992**, *33*, 5165.
- [16] H. Muerner, P. Belsler, A. von Zelewsky, *J. Am. Chem. Soc.* **1996**, *118*, 7989.
- [17] O. Mamula, A. von Zelewsky, T. Bark, H. Stoeckli-Evans, A. Neels, G. Bernardinelli, *Chem. Eur. J.* **2000**, *6*, 3575.
- [18] L. Helm, A. Borel, A. E. Merbach, *NMRICMA 2.7*, University of Lausanne, Lausanne, **2000**.
- [19] A. K. Rahimi, A. I. Popov, *Inorg. Nucl. Chem. Lett.* **1976**, *12*, 703.
- [20] E. Paci, B. Velikson, *Biopolymers* **1997**, *41*, 785.
- [21] A. Drljaca, C. D. Hubbard, R. van Eldik, T. Asano, M. V. Basilevsky, W. J. le Noble, *Chem. Rev.* **1998**, *98*, 2167.
- [22] G. Pappenberger, C. Saudan, M. Becker, A. E. Merbach, T. Kiefhaber, *Proc. Natl. Acad. Sci. USA* **2000**, *97*, 17.
- [23] M. L. Connolly, *Science* **1983**, *221*, 709.
- [24] C. Amman, P. Meier, A. E. Merbach, *J. Magn. Res.* **1982**, *46*, 319.
- [25] A. Cusanelli, L. Nicula-Dadci, U. Frey, L. Helm, A. E. Merbach, *Inorg. Chem.* **1997**, *36*, 2211.
- [26] U. Frey, L. Helm, A. E. Merbach, R. Roulet, *Advanced Applications of NMR to Organometallic Chemistry*, Wiley, New York, **1996**.

Received: August 10, 2000 [F2668]